Comprehensive testing of indoor ventilation in underground transit hubs and microclimate in adjacent sunken plazas

Chenxing Wang[1], *Xiaoyu* Zhao[1], *Jianbing* Zang[1], and *Yan* Wu[1*]

[1] School of Mechanical Engineering, Tongji University, Shanghai, 201804, China

Abstract. Transit-Oriented Developments (TODs) are widely adopted as a sustainable strategy in the rapidly urbanising world. Underground transit hubs and sunken plazas, as key components of TOD communities, significantly influence the health and comfort of pedestrians, as well as energy consumption, through the modulation of indoor and outdoor ventilation conditions. This study conducted field tests to comprehensively investigate the thermal environment, humid conditions, ventilation conditions, and air quality within these areas. The main findings include: Sunken plazas demonstrate enhanced stability in temperature and humidity fluctuations relative to their aboveground counterparts. The sunken structure contributes to wind speed attenuation, with a more pronounced reduction observed at the entrance and exit of underground transit hubs compared to the central area of the sunken plazas. The difference in temperature between indoor and outdoor environments is a key factor influencing the overall airflow direction and ventilation performance, subsequently affecting the energy consumption of mechanical ventilation systems. The concentration and distribution of particulate matter are influenced by airflow patterns and wind speed, showing an increasing gradient from aboveground spaces to indoor crowded areas. The results provide scientific evidence and practical guidance for enhancing ventilation performance and air quality in sustainable urban design.

1 Introduction

Rapid urbanization worldwide drives economic growth and social transformation but also triggers challenges such as land scarcity, ecological space reduction, increased energy consumption, and deteriorated living environment quality [1]. The strategy of Transit-Oriented Developments (TODs), as a sustainable urban planning approach, has emerged to efficiently utilize urban land, alleviate regional traffic congestion, and foster multi-functional high-density communities [2]. Underground transit hubs and adjacent outdoor sunken plazas, integrating transportation, commercial, office, and leisure entertainment functions, significantly attract foot traffic and extend visitor duration. This complexity heightens air quality management challenges and demands for occupant health and comfort [3]. The status of natural ventilation in these areas significantly affects the energy consumption and operational efficiency of mechanical ventilation and air conditioning systems. Consequently, this impacts the overall energy strategy and the effectiveness of environmental control within the TODs complexes [4].

Previous research focusing on underground transit hubs has primarily concentrated on the physical aspects of the environment. Huang et al. [5] studied the lighting and thermal environment of underground public transport hubs in Shenzhen, finding that large skylights reduce annual air conditioning energy consumption and enhance lighting performance, though requiring shading in summer to mitigate thermal discomfort for pedestrians. Zhao et al. [6] applied Particle Image Velocimetry and wind tunnel experiments to discover that indoor wind speed decreases with the height of underground transit buildings and developed a predictive model for airflow through large openings. Guan et al. [7] conducted field measurements in subway station public areas, highlighting significant outdoor airflow through entrances and related influencing factors. Regarding outdoor environments of sunken plazas, Han et al. [8] utilized numerical simulations to evaluate the challenges posed by excessive solar radiation and pollutant accumulation in these courtyards during the summer months. Their research showed that implementing shading solutions, green walls, and water features can reduce temperatures in active zones by up to 5.6°C, while the strategic placement of wind-blocking and guiding walls can substantially enhance the wind environment. Zhao et al. [3] examined the microclimate effects within subway station sunken plazas situated in subtropical regions, noting a temperature gradient from the bottom to the top of these spaces and an increasing wind attenuation effect correlating with the shape coefficient of sunken plazas. However, studies on the interconnectedness and distribution patterns between overall ventilation performance and air quality in underground transit hubs and adjacent sunken plazas are limited.

* Corresponding author: yan.wu@tongji.edu.cn

Therefore, this paper conducts a comprehensive investigation of the indoor and outdoor environments of underground transit hubs and the impact of adjacent sunken plazas, focusing on ventilation conditions and current air quality. It aims to provide scientific evidence and practical guidance for urban development in similar climatic regions, with an emphasis on enhancing resident health and life quality while promoting sustainable urban growth. This study highlights the importance of optimizing ventilation and air quality in the early design phases of emerging TOD projects, aiming to achieve an optimal balance among air quality, energy efficiency, and environmental comfort.

2 Methods and materials

2.1 Description of the testing site

This study was conducted at a representative TODs complex located in the Hongqiao Business District of Shanghai, a multifunctional urban space that integrates transportation, commerce, office space, and leisure entertainment. The structural layout of the complex, encompassing the underground transit hub, the outdoor sunken plaza, the shopping centre, and office buildings, is illustrated in Fig. 1. The entrance/exit provides direct access to the sunken plaza, situated approximately 6 m beneath ground level. The sunken plaza extends over an area, measuring 100 m in length and 50 m in width.

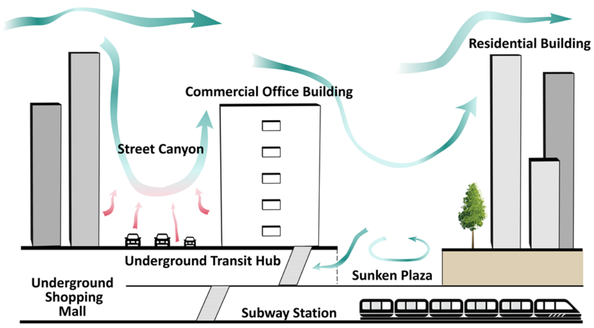

Fig. 1. Schematic of structural layout in Transit-Oriented Developments configuration.

2.2 Testing instruments and methodology

Environmental monitoring was performed across two consecutive days, January 4 and 5, 2024, spanning from 8:00 to 18:00, under clear weather conditions. The monitoring points, as depicted in Fig. 2, included the aboveground space (for background meteorological data reference), the sunken plaza centre, the entrance/exit of the underground transit hub, and the indoor crowded area. The parameters measured were air temperature, relative humidity, black globe temperature, wind speed, wind direction, and particulate matter concentration. The equipment utilized for testing is outlined in Table 1. Instruments were positioned 1.5 meters above the ground at each monitoring site, ensuring that the collected data accurately reflect the air quality conditions pedestrians are most likely to encounter.

Table 1. Measuring instruments parameters information.

Instrument	Operational Range	Resolution
Testo 400 Testo 0554 1111 Testo 0635 1571	-20-70℃ 5-95% 0-50 m/s	0.1℃ 0.1% RH 0.01 m/s
RM Young 81000	0-40 m/s 0-360°	0.01 m/s 0.1°
KIMO TM200 KIMO BN-150-45	0-60℃	0.5℃
TSI 8532	0.001-150 mg/m^3	0.001 mg/m^3
Testo 868	7.5-14 μm	0.08°C (80 mK)

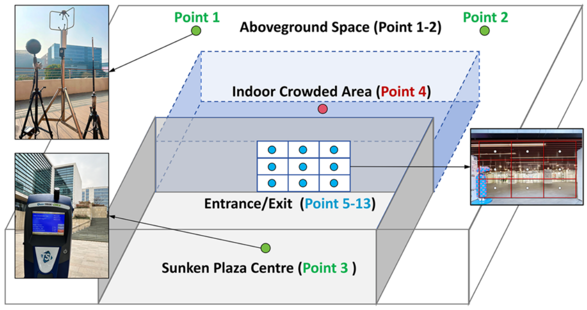

Fig. 2. Measurement points at various locations.

Air temperature, black globe temperature, relative humidity, wind speed and direction were continuously monitored, with data logging at 1-second intervals. This high-resolution data collection facilitated a detailed analysis of temporal variations in environmental conditions. Particulate matter concentrations at different locations were measured multiple times during the testing period to ensure data robustness and minimize the risk of anomalies, with each measurement session lasting 15 minutes. Additionally, thermal imaging cameras employing infrared thermography captured the temperature distribution in the space around the transit hub entrances and exits.

To further investigate the air exchange through the entrance/exit between the underground transit hub and the sunken plaza, a high-precision 3D ultrasonic anemometer (RM Young 81000) was deployed at monitoring points 5-13 to measure wind speed and direction, which were then used to calculate the corresponding airflow rates and air exchange volumes [9]. This equipment accurately captures 3D variations in wind speed and direction, providing detailed insights into airflow patterns.

3 Results and discussion

3.1 Thermal environment and humidity levels

Fig. 3 illustrates the diurnal changes in outdoor air temperature and relative humidity at the aboveground space and the sunken plaza. Both locations exhibited a consistent upward trend in temperature during the morning hours, with the aboveground space recording higher temperatures than the sunken plaza. The temperature difference between the two sites gradually widened, peaking at a maximum differential of 5.6°C between 12:40 and 13:40, before showing a decreasing trend towards 18:00, when the difference narrowed to 0.8°C. The average temperature was 15.1°C in the aboveground space and 12.7°C in the sunken plaza. The more rapid temperature increase in the aboveground space is directly related to their exposure to solar radiation, with the maximum temperature difference observed during noon when solar radiation is at its strongest. The sunken plaza experiences a slower temperature increase due to its structural design, shading from surrounding buildings, and evaporative cooling from vegetated areas. However, the trend in relative humidity across both locations is inversely correlated with temperature changes, reaching a maximum humidity difference of 15.2% between 13:00 and 14:00, slightly later than the peak temperature differential. The overall relative humidity was higher in the sunken plaza, averaging 57.8%, compared to 49.8% in the aboveground space. Vegetation contributes to local absolute humidity through transpiration, releasing water into the air, which helps maintain higher relative humidity levels even as temperatures increase. This interplay between temperature and humidity across different urban areas is crucial for understanding urban microclimate dynamics.

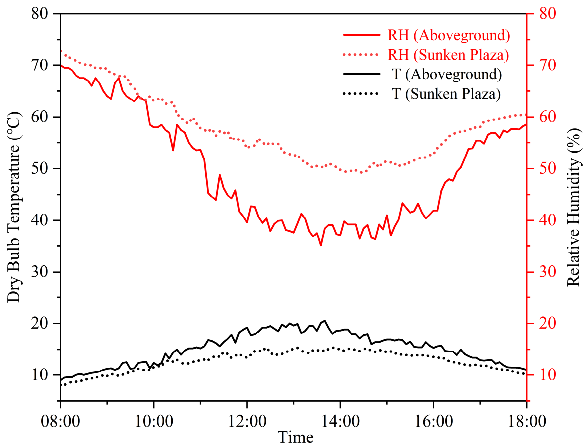

Fig. 3. Variations in temperature and relative humidity in aboveground space and sunken plaza.

Fig. 4 presents the variations in dry bulb temperature and black globe temperature observed in aboveground spaces, the sunken plaza, and indoor crowded areas. The temperature in aboveground spaces exhibited significant sensitivity to solar radiation, with the black globe temperature notably affected, reaching up to 31°C, and averaging 8.5°C higher than the dry bulb temperature. This phenomenon underscores the substantial thermal effect of solar radiation on urban microclimates. In contrast, the difference between dry bulb and black globe temperatures in the sunken plaza and the transit hub is less pronounced, with black globe temperatures exceeding dry bulb temperatures by 0.9°C and 0.4°C, respectively. The reduced disparity can be attributed to the design of the sunken plaza and surrounding buildings, which mitigate the impact of direct solar radiation. Temperatures within the underground transit hub remained relatively stable, mainly fluctuating between 16-18°C, due to the enclosed environment and the architectural design features such as insulation, ventilation, and air conditioning systems.

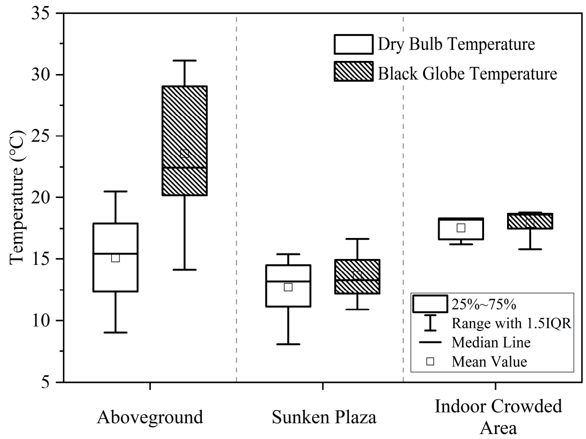

Fig. 4. Comparison of black globe temperature and dry bulb temperature at different locations.

During the winter, temperatures in the sunken plaza are notably lower than those inside the underground transit hub, resulting in a significant temperature gradient between indoor and outdoor spaces. Thermal imaging captured at the entrance, as shown in Fig. 5, illustrates this difference. The thermal gradient promotes the influx of cold air through the sunken plaza into the indoor space. While this introduces fresh air, facilitating circulation and renewal of indoor air, it also increases energy consumption as the air conditioning system counteracts the temperature drop caused by the cold air intrusion.

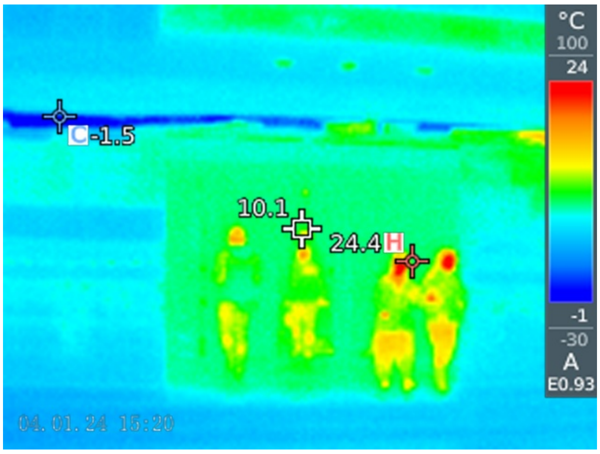

Fig. 5. Thermal imaging display of temperature distribution at entrance/exit.

3.2 Wind speed and airflow rate

Fig. 6 depicts the distribution of wind speeds at different locations, demonstrating that due to the sunken structure and obstructions from surrounding buildings, the average wind speed at the aboveground space is approximately 1.5 times greater than that at the centre of the sunken plaza.

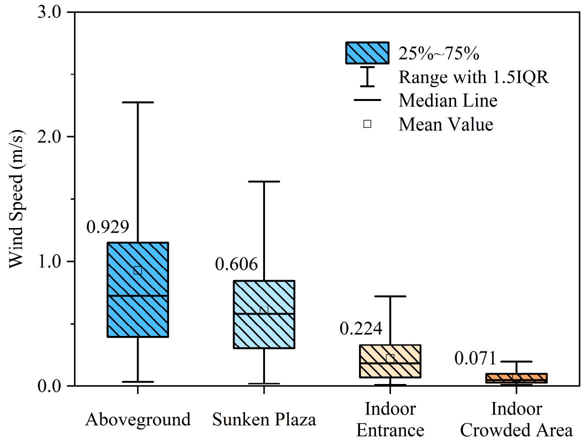

Fig. 6. Wind speed at different locations.

Furthermore, based on the wind speed and direction of nine points at the entrance/exit, as depicted in Fig. 2, the average wind speed is measured at 0.224 m/s. Equation (1) is applied for the calculation of airflow rate.

$$Q = \pm 3600 \times \sum_{i=1}^{9} v_i \bullet A_i \tag{1}$$

where Q is the net volume of air exchanged due to air movement, measured in cubic meters per hour (m^3/h), '+' represents air inflow from outdoors to indoors, and '-' represents air outflow from indoors to outdoors, 'i' is the index of each measurement point, 'v_i' represents the value of wind speed at measurement point i, and A_i represents the area at measurement point i (A_i=A/9, A is the total area).

The overall airflow at the entrance/exit of the underground transit hub is characterized by an inflow condition, where the air inflow rate from the exterior to the interior is calculated to be 1080 m^3/h. This inflow is mainly caused by the thermal pressure difference between the indoor and outdoor environments in winter, facilitating the entrance of fresh and cold air into the indoor space of the underground transit hub. The wind speed in the sunken plaza is found to be 2.7 times higher than that at the entrance of the transit hub. This difference in wind speeds is attributed to the airflow encountering more obstructions in the entrance/exit area along the façade of the sunken plaza, resulting in comparatively weaker air movement. The average wind speed in crowded areas within the underground transit hub is 0.071 m/s, which complies with the indoor wind speed limitations set by ANSI/ASHRAE Standard 55 [10], thereby preventing discomfort from excessive wind speeds.

3.3 Particulate matter distribution

Fig. 7 illustrates the distribution of total particulate matter concentrations at different locations. The monitoring results reveal significant variations in particulate matter concentrations based on location, with the aboveground space at 219 μg/m^3, the sunken plaza at 240 μg/m^3, the entrance/exit of the underground transit hub at 276 μg/m^3, and the highest concentration found at the indoor crowded area, reaching 340 μg/m^3. This distribution pattern is directly related to the decrease in wind speed, leading to the accumulation of particulate matter. Despite the more pronounced effect of outdoor wind at the entrance/exit, the activity of people moving in and out results in higher particulate matter concentrations compared to the sunken plaza. Inside the underground transit hub, human activities significantly impact particulate matter levels, as various forms of movement can resuspend settled particles, leading to higher concentrations in the air. Additionally, the indoor air circulation and ventilation systems may facilitate the dispersion of particulate matter, further complicating the dynamics of particulate matter distribution.

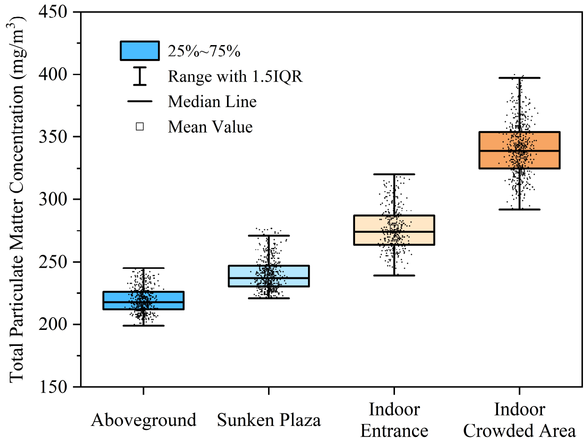

Fig. 7. Distribution of total particulate matter concentrations at different locations.

Fig. 8 shows the particulate matter concentration at four locations within various particle size ranges, demonstrating an increasing concentration trend with larger particle sizes, from PM1 to PM10. This trend is due to the cumulative nature of the measurements, which means that the assessment cumulatively includes all particulate matter with sizes not exceeding the specified thresholds. Consequently, as the maximum threshold of particle size increases, the measured total quantity of particulate matter also increases.

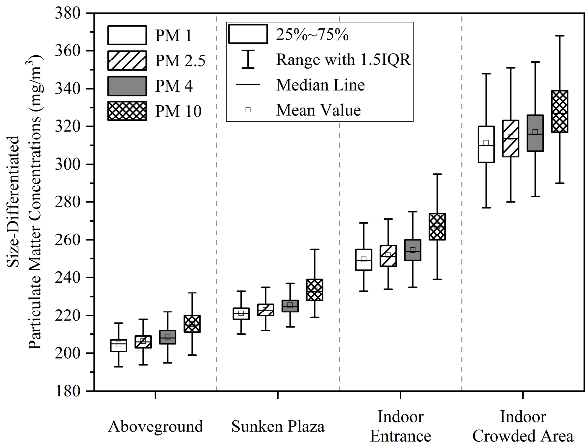

Fig. 8. Distribution of size-differentiated particulate matter concentrations at different locations.

Table 2 displays the proportions of particulate matter across various particle size ranges. Particles with a diameter of 1 μm or less consistently represent the highest proportion, approximately 90%, across different locations. Particles in the 4-10 μm range and those exceeding 10 μm in diameter make up about 4-7% of the total. Notably, particles of 1 μm or smaller constitute over 99% of the PM2.5 category, demonstrating that the overwhelming majority of PM2.5 particles are less than 1 μm in size. The predominance of smaller particles can be attributed to their lower mass, which facilitates their suspension and propagation in the air. In contrast, larger particles tend to settle more quickly due to gravitational forces, leading to distinct distribution patterns in both indoor and outdoor environments.

Table 2. Proportions of particulate matter across different particle size ranges (%).

	Above-ground	Sunken Plaza	Entrance /Exit	Indoor Crowded Area
≤1 μm	93.38	92.16	90.22	91.44
1-2.5 μm	0.80	0.75	0.86	0.93
2.5-4 μm	0.97	0.99	1.00	0.77
4-10 μm	3.14	3.44	4.56	3.19
≥10 μm	1.71	2.66	3.36	3.67

4 Conclusions

This research conducted comprehensive field tests in a typical urban TODs community, encompassing an underground transit hub and its connected sunken plaza, to assess the indoor and outdoor environments, ventilation effects, and air quality. The main findings are summarized as follows:

(1) Sunken plazas demonstrate enhanced stability in temperature and humidity fluctuations relative to their aboveground counterparts. This stability is primarily attributed to the unique architectural configurations, integrated greening strategies, and the extent of human activities within these spaces. Sunken plazas exhibit lower ambient temperatures, reduced disparity between dry bulb and black globe temperatures, and elevated relative humidity levels.

(2) The architectural design of the sunken plaza contributes to a marked attenuation in wind speed relative to that in aboveground spaces. The entrance and exit areas, which are directly linked to indoor spaces and mainly situated along the enclosed facades, exhibit significantly reduced wind speeds in comparison to the central open area of the sunken plaza.

(3) The temperature differential between the sunken plaza and the indoor spaces of the underground transit hub is a key factor affecting ventilation performance and airflow direction. The thermal pressure difference, resulting from indoor-outdoor temperature variances, facilitates air circulation and renewal but also leads to increased energy consumption in mechanical ventilation systems.

(4) The concentration and distribution of particulate matter are significantly shaped by airflow dynamics and wind speed both indoors and outdoors. Influenced by architectural configurations and pedestrian dynamics, airflow undergoes variations in both speed and direction, which in turn, directly modulate the dispersion and settlement of particulate matter. This dynamic results in particulate matter concentrations showing an increasing gradient from aboveground spaces to the sunken plaza, entrance/exit areas, and indoor crowded areas.

Acknowledgements

This work is supported by the National Natural Science Foundation of China under the project number of 52108087 and the Natural Science Foundation of Shanghai under the project number of 21ZR1467900.

References

1. Y. Qiao, F. Peng, S. Sabri, A. Rajabifard, Low carbon effects of urban underground space, Sust. Cities Soc. **45**, 451-459 (2019)
2. D. Qiang, L. Zhang, X. Huang, Quantitative Evaluation of TOD Performance Based on Multi-Source Data: A Case Study of Shanghai, Front. Public Health **10**, 820694 (2022)
3. J. Zhao, J. Dong, X. Zhang, Y. Na, C. Jiang, F. He, Q. Cui, J. Liu, Field measurement of microclimate of sunken square and its effect on indoor environment of underground metro station in subtropical region, Build. Environ. **228**, 109873 (2023)
4. A. Mukhamedjanov, T. Kidokoro, F. Seta, Y. Yang, Reshaping the concept of transit-oriented development in response to public space overheating near the transit nodes of Tokyo, Cities **116**, 103240 (2021)
5. S. Huang, S. Hao, J. Li, J. Dong, J. Liu, Effects of large skylights on lighting and thermal environments in underground public transport hubs: A case study in Shenzhen, Build. Environ. **250**, 111182 (2024)
6. J. Zhao, J. Dong, H. Gao, Z. Wang, Y. Na, C. Jiang, J. Liu, Study on airflow characteristics of underground transportation buildings with sunken squares using particle image velocimetry experiments in a wind tunnel, Build. Environ. **242**, 110469 (2023)
7. B. Guan, T. Zhang, X. Liu, Performance investigation of outdoor air supply and indoor environment related to energy consumption in two subway stations, Sust. Cities Soc. **41**, 513-524 (2018)
8. G. Han, Y. Wen, J. Leng, L. Sun, Improving Comfort and Health: Green Retrofit Designs for Sunken Courtyards during the Summer Period in a Subtropical Climate, BUILDINGS-BASEL **11**, 413 (2021)
9. K. Zhao, J. Weng, J. Ge, On-site measured indoor thermal environment in large spaces of airports during winter, Build. Environ. **167**, 106463 (2020)
10. ASHRAE, *Standard 55-2017 Thermal environment*

conditions for human occupancy, American Society of Heating, Refrigerating and Air-conditioning Engineers, Inc., Atlanta, GA, US (2017)